AJNR

Comparison of functional MR and H2 15O positron emission tomography in stimulation of the primary visual cortex.

M A Kraut, S Marenco, B J Soher, D F Wong and R N Bryan

AJNR Am J Neuroradiol 1995, 16 (10) 2101-2107
http://www.ajnr.org/content/16/10/2101

Comparison of Functional MR and $H_2{}^{15}O$ Positron Emission Tomography in Stimulation of the Primary Visual Cortex

Michael A. Kraut, Stefano Marenco, Brian J. Soher, Dean F. Wong, and R. Nick Bryan

PURPOSE: To locate spoiled gradient-echo functional MR signal changes in relation to brain parenchyma. **METHODS:** The region of the primary visual cortex was evaluated using functional MR and $H_2{}^{15}O$ positron emission tomography in each of six male subjects who were being visually stimulated by means of red light-emitting diode flash goggles. **RESULTS:** The positron emission tomography technique demonstrated substantially greater relative signal change with visual stimulation than did the functional MR technique. Furthermore, the functional MR signal changes were concentrated in loci around the periphery of brain parenchyma exhibiting increased radiotracer activity, as opposed to being collocated. **CONCLUSIONS:** Signal changes found using functional MR based on gradient-echo techniques reflect primarily phenomena occurring within small veins and underrepresent activity intrinsic to brain parenchyma, thus introducing potential inaccuracies in locating regions of activated brain tissue. Positron emission tomography, however, directly measures changes in metabolically related activity within the parenchyma.

Index terms: Magnetic resonance, functional; Positron emission tomography

AJNR Am J Neuroradiol 16:2101–2107, November 1995

During the past several years, techniques to detect magnetic resonance (MR) signal changes reflecting brain function, as opposed to simply structure, have been developed (1–3). Applications of these functional MR techniques have revealed signal changes coincident with activation of sensory (2–11) and motor (8, 11–17) cortical regions. Signal changes also have been reported with experimental paradigms designed to evaluate higher cortical function (18, 19).

Received February 8, 1995; accepted after revision May 23.

Supported in part by the Basic Science Fellowship Award from the American Society of Neuroradiology (M.A.K.), grant HD 24061 from the National Institutes of Health (D.F.W.), and a grant from the National Alliance for Research on Schizophrenia and Depression (D.F.W., S.M.).

Presented at the 32nd Annual Meeting of the American Society of Neuroradiology, Nashville, Tenn, May 1994.

From the Departments of Radiology (M.A.K., S.M., D.F.W., R.N.B.) and Biomedical Engineering (B.J.S.), Johns Hopkins University, Baltimore, Md.

Address reprint requests to Michael A. Kraut, MD, PhD, Johns Hopkins University, Division of Neuroradiology, 600 N Wolfe St, Baltimore, MD 21287-2182.

AJNR 16:2101–2107, Nov 1995 0195-6108/95/1610–2101

The signal changes themselves have been attributed to some combination of local changes in blood flow and concentration of capillary or venous deoxyhemoglobin with cerebral activation. The degree to which each of these factors contributes also is dependent on magnetic field strength and imaging parameters (repetition time, echo time, tip angle) (20).

Theoretical considerations (9, 10, 21) as well as empirical observations (22, 23) strongly suggest that the gradient refocused techniques commonly used in functional MR show signal changes disproportionately reflecting flow through small and medium-size veins, as opposed to intraparenchymal capillaries. This distinction is potentially important, because the veins draining a cortical region may overlie the activated area for only some part of their course. Thus, the accuracy of the spatial location of cortical activation afforded by these techniques is open to question.

In an attempt to provide further empirical evidence relevant to this issue, we compare the characteristics of the functional MR signal changes seen using gradient refocused techniques with $H_2{}^{15}O$ positron emission tomography (PET), a generally accepted technique for

evaluating regional cerebral blood flow (24). We have chosen to perform these studies in primary visual cortex because of the robust functional MR responses reported by many investigators in this region, as well as because of the well-documented changes in regional cerebral blood flow as measured by PET (25, 26).

Methods

Six men ranging in age from 24 to 50 years were the subjects in these studies. The protocol was approved by the institutional joint committee on clinical investigation.

Each subject was fitted with a thermoplastic mask (TRU-SCAN Imaging, Annapolis, Md) to help maintain constant head position during the MR and positron emission tomography examinations.

The MR examinations were performed on a 1.5-T system, using a standard head coil. Gross movement of the head was prevented by means of the thermoplastic mask. The imaging sequences used to define the anatomic templates on which the functional data were superimposed included sagittal T1-weighted scout images (533/11/1 [repetition time/echo time/excitations]), volume-acquired axially oriented spoiled gradient-echo images (35/5/1; tip angle, 45°; partitions, 124; 1.5-mm partition thickness), and three contiguous 4-mm-thick angled T1-weighted images angled along and centered on the long axis of the calcarine fissures of the occipital lobes. All anatomic and functional images were acquired using a 24-cm field of view and a 256 × 128 acquisition matrix. The functional MR images were acquired as three series of 4-mm-thick spoiled gradient-echo (60/40/1; tip angle, 40°) images angled along the calcarine fissure. One series was centered on the fissure, and the other two were displaced 4 mm above and below the central section. Each series consisted of 60 image acquisitions, which in turn were divided into five cycles of six images acquired with the stimulus off, alternating with six acquired with the stimulus on. Each on–off cycle lasted 72 seconds, with the total time for five cycles being 6 minutes. The stimulus was binocular red flashing light with a flash frequency of 7.8 Hz, delivered using a SV10 light-emitting diode goggle system (Grass Inc, Quincy, Mass).

PET regional cerebral blood flow data were gathered using a whole-body scanner, having 6-mm full width at half maximum inplane resolution and 6.5-mm axial resolution. During the PET examination, the subject's head was held stationary by the previously formed thermoplastic mask. Stimulation again was provided by the same red light-emitting diode goggles flashing at 7.8 Hz. Each subject underwent three bolus injections of 75 mCi of $H_2{}^{15}O$ into the antecubital fossa. In four of the subjects, two injections were made without visual stimulation to assess for stability of the baseline, and one injection was made with stimulation. In two subjects, one data set was gathered without, and two gathered with, visual stimulation. The sequence of stimulated versus nonstimulated conditions was varied across subjects to avoid order effects. During the visual stimulation sessions, the tracer was injected as a bolus at the same time that visual stimulation was started. PET data were gathered starting immediately at the time of injection and continuing for 120 seconds, with an acquisition rate of 10 seconds per frame. Retrospectively, the six frames of data gathered after significant tracer activity first appeared in the brain (typically frames 3 through 8, corresponding to 20 to 90 seconds after injection) were averaged after performing decay correction. This procedure yields a measure of activity that includes data gathered during the period of maximal tracer uptake (27) and that should thus be sensitive to flow (28). In the nonstimulated condition, data also were gathered for 60 seconds after tracer injection. PET images initially were reconstructed using a 128 × 128 matrix and a 2-mm pixel size, with a 6-mm Hann filter.

Image Processing

Both the anatomic and functional MR data sets were processed on a Sparc 10 workstation (Sun Inc, Mountain View, Calif), using both software developed in-house as well as NIH Image (National Institutes of Health, Bethesda, Md, with some modifications made at our institution; see "Acknowledgments"). To create a template on which to superimpose the functional MR and PET data, the volume spoiled gradient-echo data set was initially resampled to obtain isometric voxels (.9375 mm in each dimension), and "resectioned" to the same angle as the functional MR images. The accuracy of the result of this operation was checked by comparing the resectioned spoiled gradient-echo images depicting the calcarine fissure with the angled T1-weighted images obtained at the same locations as the functional MR data sets. These reoriented images then were averaged into 2-mm-thick sections. The PET data were subjected to the same interpolation procedure, resulting in 2-mm-thick PET images. This last operation does not increase the spatial resolution of the PET data set, but simply facilitates coregistration with the similarly processed MR sections. The PET and the anatomic MR data sets then were superimposed using the REGISTER software package (Montreal Neurological Institute, Quebec, Canada) (29, 30). This technique involves placing multiple coregistration reference points at homologous locations within each of the data sets and has been shown to facilitate coregistration to within about 2 mm in each direction (31). We typically placed between 15 and 20 of these points in the data sets of each subject. The correspondence of the final superimposed PET, anatomic MR, and functional MR sections was checked by comparing the contours of their borders, both peripherally at the cortical margins and centrally using ventricular borders, basal ganglia, and thalamic hemispheres. Typically, only minor mismatches were observed, and the contours differed by less than 1 mm radially. The initial step in processing the functional MR data was to average images 2 through 6 (first cycle, stimulus off) to create a baseline image. Image 1 of the series was not included in the calculation of the

Maximal percent signal changes (signal change-to-noise ratios) in PET and in functional MR with visual stimulation

Subject	Maximal Signal Change in PET	Maximal Signal Change in Functional MR
1	50% (4.7)	13% (1.5)
2	41% (4.5)	12% (1.4)
3	35% (3.3)	6% (1.3)
4	69% (5.9)	7% (2.6)
5	35% (2.7)	5% (1.1)
6	40% (3.6)	none detectable

baseline, because visual inspection of these first images revealed that signal from the tissue within the section had not yet reached steady-state magnetization. The baseline then was subtracted from each image, numbers 1 through 60, of the previously described on–off sequence. The subtracted images then were subjected to *z*-score analysis (32); including image 1 in the analysis did not have an appreciable affect on the signal change profiles evaluated either by the preliminary subtraction or by *z*-score analysis. The *z*-score maps, set to a threshold of $z \geq 1$, were used to guide placement of regions of interest on the subtracted functional MR images to check for the spatial distribution of signal changes related to visual stimulation. These *z*-score maps also were superimposed on the PET and the spoiled gradient-echo images in the resectioned data set corresponding to the locations at which the data were gathered.

To compare the magnitudes of the signal change (ΔS) observed in selected region of interest with each of the two techniques, we calculated percent signal change using the formula

$$\Delta S = [(\text{Signal}_{\text{Activation}} - \text{Signal } \overline{\text{Baseline}})/\text{Signal } \overline{\text{Baseline}}]*100$$

where $\overline{\text{Baseline}}$ is the average of two baseline data sets. For each region of interest, the measure reflecting signal change-to-noise ratio (SNR) was calculated as the ratio of the mean signal increase in the activated region divided by the pixel-by-pixel standard deviation of the difference between two images obtained in the nonstimulated state:

$$\text{SNR} = [\mu\ (_{\Delta S \text{ in activated region}})/\sigma\ (_{\text{baseline1}-\text{baseline2}})].$$

Results

In each of the six subjects, the maximal increase in signal with visual stimulation was much greater in the regional cerebral blood flow PET data than in the functional MR data (Table). In one of our subjects (subject 6), no functional MR signal changes were observed, although substantial (up to 40%) regional cerebral blood flow changes were detected by PET with visual stimulation. The signal change-to-noise ratios were better for the PET studies as well, varying between two and four times those seen during the functional MR studies performed on the same subject.

Representative functional MR data from one subject are depicted in Figure 1. The *z*-score map shows that the loci of consistent signal increase are curvilinear and are mostly collocated with sulci. A region of interest placed over one of these sulci reveals signal changes of 8% to 10% above baseline with visual stimulation. In contrast, the same-size region of interest displaced less than 3 mm, but still overlying calcarine cortex, shows no discernible signal changes. Superimposition of the functional MR and the PET data sets (Fig 2) also indicates that the regions of functional MR signal increase for the most part do not overlie the cortex itself, but appear to marginate partially the areas of calcarine cortex, which exhibit the greatest increase in PET regional cerebral blood flow. The separations between any individual functional MR signal change and associated PET regional cerebral blood flow changes closely relate to the quite variable distance between the parenchyma exhibiting the blood flow increase and the nearest sulcus. Also, we observed many cortical regions that demonstrated maximal or near maximal increases in PET regional cerebral blood flow with visual stimulation but virtually no regional functional MR signal increases.

Discussion

Although several previously published studies have shown convincingly the spatial correspondence of gradient-echo functional MR signal changes to the locations of small superficial vessels, our data explicitly demonstrate the variable spatial relationship between the functional MR signal changes and the $H_2{}^{15}O$ PET–measured regions of change in cerebral cortical blood flow, which presumably relate to changes in regional neuronal activity. Comparison of the tabulated PET and functional MR data also clearly demonstrates the significantly greater relative signal change afforded by the blood flow PET technique compared with those seen with gradient refocused functional MR. Additionally, the wide spatial distribution of the PET signal changes within the occipital cortex, an expected finding given the diffuse nature of the stimulus, contrasts markedly with the sharply circumscribed nature of the functional MR signal-change distribution. These differences

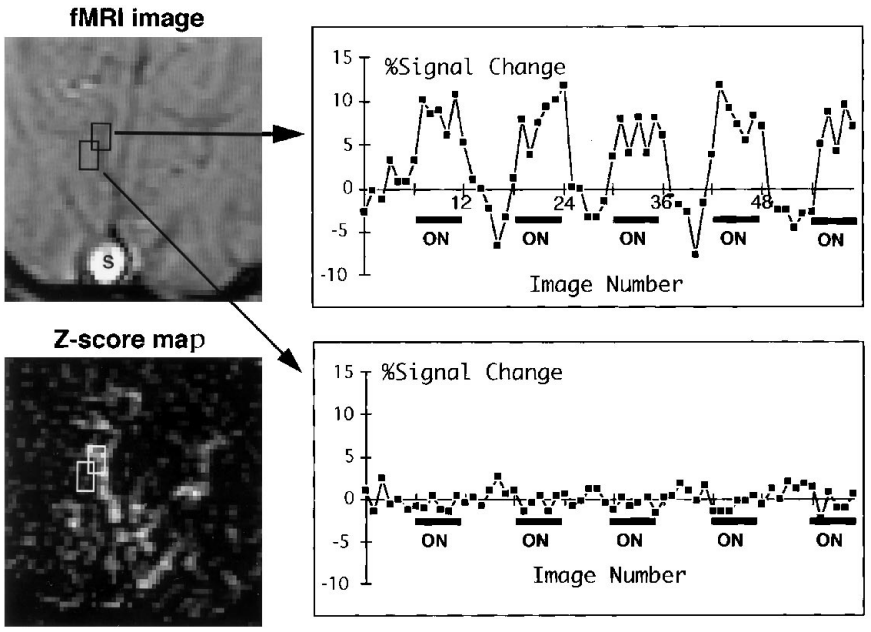

Fig 1. Comparison of functional MR (*fMRI*) signal changes overlying sulcus with those overlying adjacent calcarine cortex. Image in lower left is *z*-score map centered over occipital region, which was used to guide the placement of the regions of interest on the subtracted image (*upper left*). Corresponding regions of interest are shown on both the *z*-score map and the subtracted image. Signal changes overlying sulcus (more anteromedial region of interest) were robust and closely followed the stimulus on-off cycle; signal changes overlying the subjacent cortex (posterolateral region of interest) were virtually undetectable. *On* intervals correspond with the times during which the light-emitting diode goggles were flashing. *S* in upper left panel overlies sagittal sinus.

presumably reflect to a large degree the distinction between a technique sensitive to parenchymal changes (PET regional cerebral blood flow) and one that is apparently dominated by changes occurring within regional blood vessels (gradient-echo functional MR).

Some elements of the apparent broader distribution of the PET-estimated blood flow change than the functional MR findings may relate to the intrinsic spatial resolution of the PET data themselves. Factors such as scatter, as well as filtering/reconstruction algorithms, also might potentially contribute to inaccurate superimposition of PET signal changes on regions of activated tissue (and are the cause of the apparent slight extension of PET signal changes outside the calvarium in Figure 2B). However, we did not find these factors to influ-

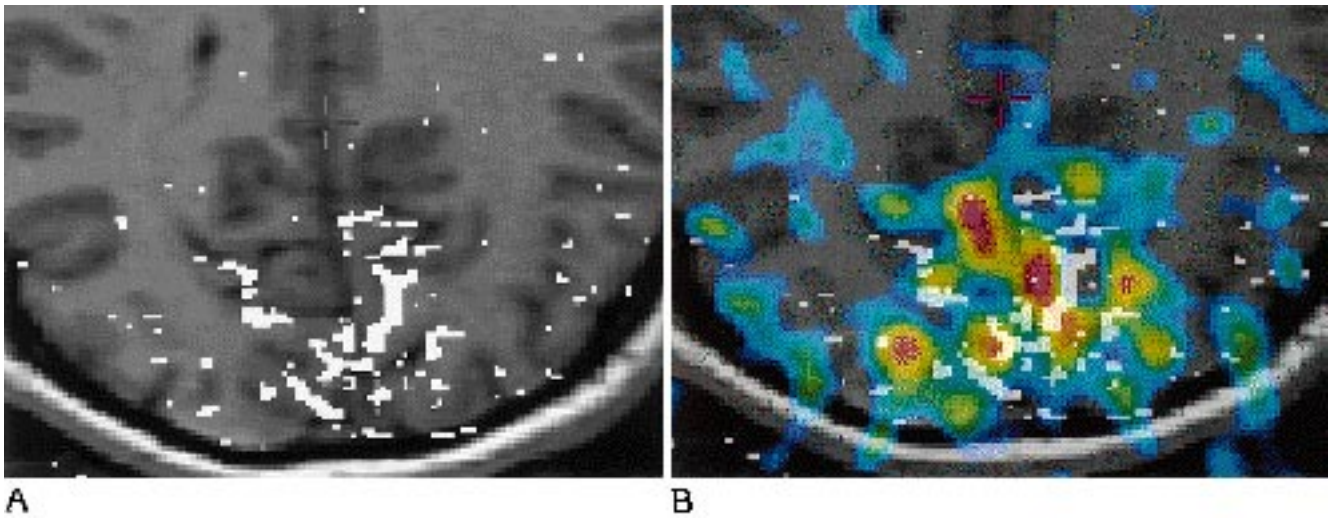

Fig 2. *A*, *Z*-score map superimposed on the corresponding MR anatomic image of calcarine cortex.

B, Superimposed *z*-score map and PET data from same section, and the spatial relationship between the signal changes detected with each technique. The loci of dominant functional MR signal change typically marginate the regions of maximal PET tracer uptake, although some regions exhibiting large changes in parenchymal blood flow demonstrate little if any adjacent functional MR signal change. Highest activity in PET data are shown in red, with orange, yellow, green, and blue, respectively, reflecting lower levels of measured regional blood flow. Regions of PET signal projecting outside the MR-defined boundaries of the head reflect data filtering and reconstruction processes. This is a different data set from that shown in Figure 1.

ence substantially the location of the activity, because the PET signal-change maxima are all deep to (ie, on the parenchymal side of) the loci of functional MR signal changes. Significant inaccuracy presumably would result in apparent location of at least some PET signal maxima to the sulcal, as opposed to the parenchymal, side of the functional MR changes. Similarly, we can exclude gross lateral or anteroposterior misregistration of the data sets, because such inaccuracy would be expected to cause a global and thus recognizable shift of one of the data sets relative to the other; we saw no such effects. In general, accuracy of superimposition was greatly aided by the requirement of the data coregistration software for operator placement of multiple widely distributed reference points. By placing many of these both peripherally and centrally, we were able to decrease markedly the effects of data spatial resolution and reconstruction factors on superimposition.

In our experimental condition, spatial location of the activated cortex was not in question, in that the location of primary visual cortex has long been known. Further, the stimulus used resulted in diffuse activation of the primary visual cortex. Thus, we were not depending on the spatial distribution of the functional MR signal changes to help in locating regions of cortical activation. Similarly, few if any of the published functional MR studies depend primarily on the functional MR signal changes for precise location of the activated regions; the spatial distribution of the observed signal changes typically are used to confirm functional location that has been previously documented or predicted using other experimental techniques (4, 5, 14, 18, 19, 33). In experimental circumstances under which the distribution of cortical activation is not known, location of cortical activation on the basis of the spatial distribution of gradient echo–based functional MR signal changes may lead to spurious results, in that the paths taken by the small regional veins contributing to the signal changes may not consistently overlie the regions of activated tissue. This is relevant because many investigators will not have access to MR instruments with a field strength of greater than 1.5-T, and at this field strength, readily implemented gradient-echo techniques yield signal changes that are much easier to detect than those seen with spin-echo sequences. A possible solution is the use of a technique such as statistical parametric mapping (28), which is being used with increasing frequency in PET brain activation studies. This technique facilitates location of regions of brain activation across subjects, and thus may average out the effects of disparities between the spatial distribution of activated tissue and draining vessels. The potential tradeoff here is the loss of spatial resolution intrinsic to superimposition of functional data sets from many individuals on a standardized anatomic template.

Although not displayed in their entirety, the complete PET data sets covered much of the cerebrum, whereas the functional MR data were gathered at predetermined locations. PET studies such as this one thus offer the potential for unbiased sampling of activity in a much larger volume of brain tissue. In comparison, the limited spatial sampling allowed by the most commonly used single-section functional MR techniques precludes looking for coincident or correlated signal changes in widely separated noncoplanar regions of the brain, especially in regions where one is not expecting to find them. Clearly, however, the potential of newer techniques, such as echo planar imaging or other recently reported multisection functional MR techniques (7, 34), to facilitate rapid multisection functional MR studies and thus to address the location sampling bias problems inherent in single-section techniques has yet to be explored systematically.

The apparent shortcomings of spoiled gradient echo–based functional MR techniques, whether single section or multisection, for accurate location of brain parenchymal activation suggest the need for independent means of locating areas of activated neural tissue. Depending on the experimental circumstances and the time course of neuronal activation, these means may include PET, single photon emission computed tomography, electroencephalography, evoked potentials, or magnetoencephalography (35) (Belliveau J, Baker J, Kwong K, et al, "Functional Neuroimaging Combining fMRI, MEG, and EEG," presented at the 12th Annual Meeting of the Society of Magnetic Resonance in Medicine, New York, NY, August 14–20, 1993). These techniques, including functional MR, each afford different degrees of temporal and spatial resolution and are thus potentially complementary. Functional MR techniques using fast spin-echo (7) or the recently described EPISTAR (echo planar imaging and signal targeting with alternating radio frequency) (36)

technique appear to reflect more accurately the contribution of intracapillary blood to regional signal changes. The EPISTAR technique, especially, yields very large signal changes, even at 1.5 T. Higher-field-strength MR instruments (greater than the 1.5-T unit used in this and in many of the other published studies) also confer an advantage in locating readily detectable signal changes to intraparenchymal microvasculature (9), especially when spin-echo techniques are used. Close comparison of findings made using these new and evolving functional MR techniques with those made with other (non-MR) locating methods will likely result in increased appreciation of the roles each modality has in the clinical and the basic neurosciences.

Acknowledgments

We thank Robert Dannals, PhD, and Hayden Ravert, PhD, for radiochemistry assistance in ^{15}O water production; Steven Breiter, MD, for help in production of the figures; and Alan L. Reiss, MD, of the Kennedy-Krieger Institute, Johns Hopkins University, Baltimore, Md, who provided a modified version of NIH Image. This modification was supported by grant HD 31715-01 from the National Institutes of Health.

References

1. Kwong KK, Belliveau JW, Chesler DA, et al. Dynamic magnetic resonance imaging of human brain activity during primary sensory stimulation. *Proc Natl Acad Sci USA* 1992;89:5675–5679
2. Ogawa S, Tank DW, Menon R, et al. Intrinsic signal changes accompanying sensory stimulation: functional brain mapping with magnetic resonance imaging. *Proc Natl Acad Sci USA* 1992;89:5951–5955
3. Menon RS, Ogawa S, Kim SG, et al. Functional brain mapping using magnetic resonance imaging: signal changes accompanying visual stimulation. *Invest Radiol* 1992;27:S47–53
4. Belliveau JW, Kwong KK, Kennedy DN, et al. Magnetic resonance imaging mapping of brain function: human visual cortex. *Invest Radiol* 1992;27:S59–65
5. Binder JR, Rao SM, Hammeke RA, et al. Functional magnetic resonance imaging of human auditory cortex. *Ann Neurol* 1994;35:662–672
6. Blamire AM, Ogawa S, Ugurbil K, et al. Dynamic mapping of the human visual cortex by high-speed magnetic resonance imaging. *Proc Natl Acad Sci USA* 1992;89:11069–11073
7. Constable RT, Kennan RP, Puce A, McCarthy G, Gore JC. Functional NMR imaging using fast spin echo at 1.5 T. *Magn Reson Med* 1994;31:686–690
8. Constable RT, McCarthy G, Allison T, Anderson AW, Gore JC. Functional brain imaging at 1.5 T using conventional gradient echo MR imaging techniques. *Magn Reson Imaging* 1993;11:451–459
9. Menon RS, Ogawa S, Tank DW, Ugurbil K. 4 Tesla gradient recalled echo characteristics of photic stimulation-induced signal changes in the human primary visual cortex. *Magn Reson Med* 1993;30:380–386
10. Ogawa S, Menon RS, Tank DW, et al. Functional brain mapping by blood oxygenation level-dependent contrast magnetic resonance imaging: a comparison of signal characteristics with a biophysical model. *Biophys J* 1993;64:803–812
11. Ugurbil K, Garwood M, Ellermann J, et al. Imaging at high magnetic fields: initial experiences at 4 T. *Magn Reson Q* 1993;9:259–277
12. Bandettini PA, Jesmanowicz A, Wong EC, Hyde JS. Processing strategies for time-course data sets in functional MRI of the human brain. *Magn Reson Med* 1993;30:161–173
13. Bandettini PA, Wong EC, Jesmanowicz A, Hinks RS, Hyde JS. Spin-echo and gradient-echo EPI of human brain activation using BOLD contrast: a comparative study at 1.5 T. *NMR Biomed* 1994;7:12–20
14. Cao Y, Towle VL, Levin DN, Balter JM. Functional mapping of human motor cortical activation with conventional MR imaging at 1.5 T. *J Magn Reson Imaging* 1993;3:869–875
15. Kim SG, Ashe J, Georgopoulos AP, et al. Functional imaging of human motor cortex at high magnetic field. *J Neurophysiol* 1993;69:297–302
16. Rao SM, Binder JR, Bandettini PA, et al. Functional magnetic resonance imaging of complex human movements. *Neurology* 1993;43:2311–2318
17. Schad LR, Wenz F, Knopp MV, Baudendistel K, Muller E, Lorenz WJ. Functional 2D and 3D magnetic resonance imaging of motor cortex stimulation at high spatial resolution using standard 1.5 T imager. *Magn Reson Imaging* 1994;12:9–15
18. McCarthy G, Blamire AM, Rothman DL, Gruetter R, Shulman RG. Echo-planar magnetic resonance imaging studies of frontal cortex activation during word generation in humans. *Proc Natl Acad Sci USA* 1993;90:4952–4956
19. McCarthy G, Blamire AM, Puce A, et al. Functional magnetic resonance imaging of human prefrontal cortex activation during a spatial working memory task. *Proc Natl Acad Sci USA* 1994;91:8690–8694
20. Frahm J, Merboldt KD, Hanicke W, Kleinschmidt A, Boecker H. Brain or vein—oxygenation or flow? On signal physiology in functional MRI of human brain activation. *NMR Biomed* 1994;7:45–53
21. Kennan RP, Zhong J, Gore JC. Intravascular susceptibility contrast mechanisms in tissues. *Magn Reson Med* 1994;31:9–21
22. Lai S, Hopkins AL, Haacke EM, et al. Identification of vascular structures as a major source of signal contrast in high resolution 2D and 3D functional activation imaging of the motor cortex at 1.5T: preliminary results. *Magn Reson Med* 1993;30:387–392
23. Segebarth C, Belle V, Delon C, et al. Functional MRI of the human brain: predominance of signals from extracerebral veins. *Neuroreport* 1994;5:813–816
24. Raichle ME, Martin WR, Herscovitch P, Mintun MA, Markham J. Brain blood flow measured with intravenous H2(15)O, II: implementation and validation. *J Nucl Med* 1983;24:790–798
25. Fox PT, Raichle ME. Stimulus rate dependence of regional cerebral blood flow in human striate cortex, demonstrated by positron emission tomography. *J Neurophysiol* 1984;51:1109–1120
26. Fox PT, Miezin FM, Allman JM, Van Essen DC, Raichle ME. Retinotopic organization of human visual cortex mapped with positron-emission tomography. *J Neurosci* 1987;7:913–922
27. Volkow N, Mullani N, Gould L, Adler S, Gatley S. Sensitivity of measurements of regional brain activation with oxygen-15-water and PET to time of stimulation and period of image reconstruction. *J Nucl Med* 1991;32:58–61
28. Frackowiak RS, Friston KJ. Functional neuroanatomy of the human brain: positron emission tomography—a new neuroanatomical technique. *J Anat* 1994;184:211–225

29. Evans A, Marrett S, Collins L, Peters T. Anatomical-functional correlative analysis of the human brain using three dimensional imaging systems. *Proc SPIE-MI III* 1989;1092:264–274
30. Evans AC, Marrett S, Torrescorzo J, Ku S, Collins L. MRI-PET correlation in three dimensions using a volume-of-interest (VOI) atlas. *J Cereb Blood Flow Metab* 1991;11:A69–78
31. Neelin P, Crossman J, Hawkes DJ, Ma Y, Evans AC. Validation of an MRI/PET landmark registration method using 3D simulated PET images and point simulations. *Comput Med Imaging Graph* 1993;17:351–356
32. Le Bihan D, Turner R, Zeffiro TA, Cuenod CA, Jezzard P, Bonnerot V. Activation of human primary visual cortex during visual recall: a magnetic resonance imaging study. *Proc Natl Acad Sci USA* 1993;90:11802–11805
33. Rueckert L, Appollonio I, Grafman J, et al. Magnetic resonance imaging functional activation of left frontal cortex during covert word production. *J Neuroimaging* 1994;4:67–70
34. Duyn JH, Mattay VS, Sexton RH, et al. 3-dimensional functional imaging of human brain using echo-shifted FLASH MRI. *Magn Reson Med* 1994;32:150–155
35. Jack C Jr, Thompson RM, Butts RK, et al. Sensory motor cortex: correlation of presurgical mapping with functional MR imaging and invasive cortical mapping. *Radiology* 1994;190:85–92
36. Edelman RR, Siewert B, Darby DG, et al. Qualitative mapping of cerebral blood flow and functional localization with echo-planar MR imaging and signal targeting with alternating radio frequency. *Radiology* 1994;192:513–520